

# Stimulated Raman scattering of cnoidal waves

V A Aleshkevich, V A Vysloukh, Ya V Kartashov

**Abstract.** Specific features of SRS conversion of multisoliton periodic cnoidal waves into high-energy cnoidal waves at the Stokes frequency falling within the range of anomalous group-velocity dispersion are investigated. Dependences of the maximum compression degree of the pump pulse and the characteristic distance of Stokes-wave excitation on the energy localisation parameter of the cnoidal pump wave are presented.

**Keywords:** solitons, Raman scattering, cnoidal waves.

## 1. Introduction

A class of periodic soliton solutions consisting of cnoidal waves [1–4] plays an important role for cubic media. A concept of cnoidal waves is rather appealing, since it allows the dynamics of propagation to be analysed for both single- and multicomponent periodic solutions to the nonlinear Schrödinger equation for different localisation degrees of the wave-field energy. One of the most important specific features of cnoidal waves is that, in the limiting case of strongly localised energy of the wave field, a cnoidal wave is transformed into localised bright and dark solitons [3, 5]. Note that sequences of soliton pulses rather than single soliton pulses should be usually considered in fibreoptic communication lines. A cnoidal wave may serve as a model of a sequence of optical signals, with the duty ratio being determined by the localisation degree of the wave-field energy.

One of the most natural ways to improve the rate of data transmission along a fibre-optic line is to employ soliton effects for compressing pulses in a sequence. An anomalous group-velocity dispersion allows an optical fibre to play the role of a distributed compressor [6–8]. The propagation of a multisoliton pulse under these conditions is accompanied by a periodic self-compression. At the point of maximum compression, a pulse has a form of a narrow central peak against a background of a broad pedestal. The increase in the compression ratio in such a situation leads to a decrease in the energy carried by the central peak due to a growth of the pedestal. The authors of [9, 10] have demon-

strated the possibility of using stimulated Raman scattering (SRS) for transforming a bound state of solitons (a multi-soliton pulse) at the pump frequency into a high-energy single-soliton pulse at the Stokes frequency lying within the range of anomalous group-velocity dispersion. This transformation is accompanied by a considerable compression of a localised Stokes pulse in the absence of a pedestal.

The interaction of pulses in a sequence has a considerable influence on the dynamics of SRS. Investigation of SRS of periodic cnoidal waves is of undeniable interest in this context. Such an investigation is the main purpose of this paper. The main emphasis in our analysis will be focused on the maximum compression ratio of the pump pulse and the dependence of the distance of Stokes-signal excitation on the localisation degree of the wave-field energy.

## 2. Theoretical model

In the simplest case of interaction of the pump and the first Stokes component (signal) propagating in different modes, the dynamics of generation of SRS pulses is governed by the following set of nonlinear equations [9, 10]:

$$\begin{aligned} i \frac{\partial q_p}{\partial \xi} &= \frac{1}{2} \text{sign } \beta_p \frac{\partial^2 q_p}{\partial \eta^2} - q_p (|q_p|^2 + 2|q_s|^2) - i\alpha \frac{\omega_p}{\omega_s} q_p |q_s|^2, \\ i \frac{\partial q_s}{\partial \xi} + i\delta \frac{\partial q_s}{\partial \eta} &= \frac{\sigma}{2} \text{sign } \beta_s \frac{\partial^2 q_s}{\partial \eta^2} - \frac{\omega_p}{\omega_s} q_s (|q_s|^2 + 2|q_p|^2) \\ &+ i\alpha q_s |q_p|^2, \end{aligned} \quad (1)$$

where  $q_{p,s}(\eta, \xi) = A_{p,s}(\eta, \xi)(L_{\text{dis}}/L_{\text{psm}})^{1/2}/I_0^{1/2}$  are the dimensionless complex amplitudes of the pump and signal light fields;  $A_{p,s}(\eta, \xi)$  are the slowly varying envelopes of the pump and signal fields;  $I_0$  is the intensity of the input pump pulse;  $\xi = (t - z/v_p)/t_0$  is the coordinate defined as the normalised running time related to the pump pulse;  $t_0$  is the characteristic pump pulse duration;  $v_{p,s} = (\partial k_{p,s}/\partial \omega)^{-1}$  are the group velocities of the pump and the signal;  $k_{p,s}$  are the wave numbers of the pump and signal pulses;  $\omega_{p,s}$  are the central frequencies in the spectra of the pump and the signal;  $\xi = z/L_{\text{dis}}$  is the normalised propagation coordinate;  $L_{\text{dis}} = t_0^2/|\beta_p|$  is the dispersion length corresponding to the pulse duration  $t_0$ ;  $\beta_{p,s} = \partial^2 k_{p,s}/\partial \omega^2$ ;  $L_{\text{psm}} = 2n_p/(k_p n_2 I_0)$  is the length of self-phase modulation;  $n_p$  is the unperturbed refractive index at the pump frequency;  $n_2$  is the nonlinear coefficient;  $\alpha = L_{\text{psm}}/L_{\text{amp}}$  is the amplification coefficient;  $L_{\text{amp}} = [g(\omega_s)I_0]^{-1}$  is the amplification length;  $g(\omega_s)$  is the gain at the centre of the Raman line;  $\delta = L_{\text{dis}}/L_{\text{group}}$  is the

V A Aleshkevich, V A Vysloukh, Ya V Kartashov Department of Physics, M V Lomonosov Moscow State University, Vorob'evy gory, 119899

Received 13 September 2000; revision received 18 January 2001

Kvantovaya Elektronika 31 (4) 327–332 (2001)

Translated by A M Zheltikov

group-delay parameter;  $L_{\text{group}} = v_p v_s t_0 / (v_p - v_s)$  is the group-delay length;  $\sigma = |\beta_s / \beta_p|$ .

The set of equations (1) has an integral

$$\int_{-T/2}^{T/2} (\omega_s q_p q_p^* + \omega_p q_s q_s^*) d\eta = \text{const}, \quad (2)$$

which expresses energy conservation, with the period  $T \rightarrow \infty$  for localised solutions and remaining finite in the case of periodic solutions. The first terms on the right-hand sides of equations in the set (1) describe the dispersion spreading of the pump and signal pulses. The sign of the dispersion term is positive within the range of normal dispersion (for  $\lambda < \lambda_{\text{cr}} \approx 1.3 \mu\text{m}$  in quartz fibres) and negative within the range of anomalous dispersion (for  $\lambda > \lambda_{\text{cr}}$ ). The second terms in these equations describe self- and cross-phase modulation. The last term on the right hand sides of these equations is responsible for the Raman amplification of a weak signal in the field of a high-power pump wave. The mismatch of the group velocities of the pump and the signal is included in the last term on the left-hand side of the second equation in the set (1).

The main physical processes determining the dynamics of SRS solitons can be divided into intramode and intermode processes. In the regime of anomalous dispersion, intramode processes – self-phase modulation and dispersion spreading – give rise to periodic changes in the envelope of a multisoliton pulse, manifested as a sequential compression, broadening, and splitting of the pulse into fragments. The intensity of energy exchange between the pump and the signal increases with increasing amplitude of the pump pulse.

In the regime of maximum pump pulse compression, intermode energy exchange results in the formation and subsequent avalanche-like amplification of the signal pulse. Cross-modulation wave interaction also contributes to pulse compression, accelerating energy exchange. In the case of pump depletion, the intramode self-action of the signal pulse plays a dominant role, leading to soliton formation. It is of particular interest to consider Raman amplification in the regime of anomalous dispersion, when the joint action of dispersion and nonlinear effects results in an especially considerable compression of the pump and signal pulses.

We consider excitation of Raman solitons by a pump pulse with an intensity  $I_0 \sim 1.6 \times 10^8 \text{ W cm}^{-2}$  and pulse duration  $t_0 = 500 \text{ fs}$  around the minimum of optical losses in a silica fibre at  $\lambda_p = 1.55 \mu\text{m}$  and  $\lambda_s = 1.67 \mu\text{m}$ . Within the chosen wavelength range, we have  $\beta_p \approx -2.6 \times 10^{-28} \text{ s}^2 \text{ cm}^{-1}$ ,  $\beta_s \approx -3.8 \times 10^{-28} \text{ s}^2 \text{ cm}^{-1}$ ,  $n_2 = 3.2 \times 10^{-16} \text{ cm}^2 \text{ W}^{-1}$ , and  $g \approx 6.8 \times 10^{-12} \text{ cm W}^{-1}$ . The characteristic lengths are  $L_{\text{dis}} = L_{\text{psm}} = L_{\text{amp}} = 9.62 \text{ m}$  and  $L_{\text{group}} = 0.19 \text{ m}$ , which corresponds to  $\alpha = 1$ ,  $\sigma = 1.46$ , and  $\delta = 52$ . In a double-mode optical fibre, the group velocities of the pump and the signal can be matched due to the waveguide dispersion (dependence of the characteristic group-delay length for different modes on the wave number  $V = k_p a (2n_p \delta n)^{1/2}$ , where  $a$  is the radius of the fiber core,  $\delta n$  is the difference of the refractive indices of the core and the cladding). Specifically, when the signal propagates in the  $\text{LP}_{01}$  mode and the pump propagates in the  $\text{LP}_{11}$  mode, the group velocities are matched at  $V = 4$ . The latter circumstance allows us to analyse the dynamics of generation of Raman solitons for different values of the group-delay parameter  $\delta$  including the case of group-velocity matching with  $\delta = 0$ , which is of particular interest from the theoretical viewpoint.

In the regime of anomalous dispersion, the set of equations (1) in the absence of Raman gain with a zero Stokes component,  $q_s = 0$  and  $q_p = q$ , is reduced to the cubic Schrödinger equation [1–3], which describes the profiles of solitons in a medium with a Kerr nonlinearity. Periodic solutions to this equation are well known and are given by elliptic Jacobi functions:

$$\begin{aligned} q_{\text{dn}}(\eta, \xi) &= \text{dn}(\eta, k) \exp \left[ i \xi \left( 1 - \frac{k^2}{2} \right) \right], \\ q_{\text{cn}}(\eta, \xi) &= \text{cn}(\eta, k) \exp \left[ i \xi \left( k^2 - \frac{1}{2} \right) \right], \end{aligned} \quad (3)$$

where  $k$  is the localisation parameter. The first of these solutions (the dn wave) corresponds to a wave field where oscillations along the  $\eta$  axis are superimposed on a constant component. The period of these oscillations is equal to  $2K(k)$ , where  $K(k)$  is the elliptic integral of the first kind. The second solution (the cn wave) corresponds to an oscillating field with no constant component with a spatial period equal to  $4K(k)$ . Maximum localisation for the waves of both types is achieved for  $k = 1$ . In this case, the solutions given by Eqn (3) coincide with each other, having a form of a bright soliton,  $q_{\text{dn}} = q_{\text{cn}} = \text{sech } \eta \exp(0.5i\xi)$ .

In this paper, we consider SRS of  $N$ -soliton pump waves  $Nk\text{cn}(\eta, k)$  and  $N\text{dn}(\eta, k)$  (where  $N$  is an integer), leading to the formation of cnoidal waves at the Stokes frequency. In a real experiment, the Stokes wave may build up from spontaneous noise distributed over the fibre length [11]. However, in the numerical simulation of SRS, it is more convenient to introduce a seed signal in the form  $q_s(\eta, \xi = 0) = \mu q_p(\eta, \xi = 0)$ , where the intensity of the signal wave is proportional to  $\mu^2$ , and  $\mu \ll 1$  is the relative amplitude of the seed signal. Such a formulation of the problem corresponds to the regime of a Raman amplifier. This regime is of special interest due to the fact that, by varying the amplitude of the seed signal, we can search for the regimes optimal from the viewpoint of pulse compression. Such a situation can be easily implemented in experiments by splitting a pump pulse into two channels.

In one of the channels (segments of an optical fibre), a seed signal is generated from spontaneous noise under the action of a part of the pump pulse. This seed signal is then coupled (with controllable attenuation and filtering, if necessary) into the second fibre segment synchronously with the remaining part of the pump pulse. In such a situation, the relative amplitude of the seed signal (the quantity  $\mu$ ) can be varied within a broad range by changing the fraction of energy of the pump pulse coupled into each of the channels and by adjusting the attenuation degree of the signal, the length of the first fibre segment, and the intensity of the pump itself.

### 3. Self-compression and SRS of a cn wave

Consider the self-compression and SRS of an  $N$ -soliton cn wave  $Nk\text{cn}(\eta, k)$ . The intensity of intermode energy exchange leading to the amplification of the signal wave is highly sensitive to the compression ratio of the pump pulse. With an appropriate choice of the initial conditions (small amplitudes of the seed signal), the influence of energy exchange on the self-compression dynamics of the pump pulse remains insignificant up to the point of maximum compression. The approximation of a finite number of

harmonics can be employed to describe the evolution of a multisoliton cn wave for small  $k$  in this case. This approximation is justified by the fact that, in the limiting case of a low localisation degree ( $k \rightarrow 0$ ), a cn wave is transformed into a  $k \cos \eta$  wave. With a growth in  $k$ , the spectrum of the wave is enriched with higher order harmonics rather slowly. This can be seen from the Fourier spectral expansion of the cn wave:

$$Nkcn(\eta, k) = \frac{2\pi N}{K(k)} \times \sum_{m=0}^{\infty} g^{m+0.5} (1 + g^{2m+1})^{-1} \cos \frac{(2m+1)\pi}{2k(k)}, \quad (4)$$

where  $g(k) = \exp[-\pi K'(k)/K(k)]$  and  $K'(k)$  is the complementary elliptic integral of the first kind. The parameter  $g$  rapidly decreases with  $k \rightarrow 0$ . The ratio of the amplitudes of the third, second, and first harmonics in the expansion (4) for  $k = 0.5$ , for example, is 1:56:3041. For an adequate description of the self-compression of the pump pulse, we should consider the evolution of at least four first harmonics with the frequencies  $\pm(1/2)\pi K^{-1}(k)$  and  $\pm(3/2)\pi K^{-1}(k)$ . In the spectral representation, pulse self-compression corresponds to the phase locking of two lowest order harmonics with the frequency  $\omega_1 = \pm(1/2)\pi K^{-1}(k)$  with two higher order harmonics with the frequency  $3\omega_1 = \pm(3/2)\pi K^{-1}(k)$  in the presence of energy exchange between these harmonics. Within the framework of this approximation, the wave field can be written as

$$q(\eta, \xi) = a_{3\text{low}}(\xi) \exp(-3i\omega_1\eta) + a_{1\text{low}}(\xi) \exp(-i\omega_1\eta) + a_{1\text{high}}(\xi) \exp(i\omega_1\eta) + a_{3\text{high}}(\xi) \exp(3i\omega_1\eta). \quad (5)$$

A periodic wave described by Eqn (5) contains more than 95% of energy of the corresponding cnoidal wave for  $k = 0 - 0.9$ . The amplitudes of all the harmonics at the input of the nonlinear medium are described by real quantities.

Substituting Eqn (5) into the nonlinear Schrödinger equation and equating the terms with equal frequencies, we arrive at a set of four coupled equations for harmonic amplitudes. However, using the energy-conservation law,  $|a_{1\text{low}}|^2 + |a_{3\text{low}}|^2 + |a_{1\text{high}}|^2 + |a_{3\text{high}}|^2 = b = \text{const}$ , and the Manley–Rowe relations,  $|a_{1\text{low}}|^2 - |a_{1\text{high}}|^2 = 0$  and  $|a_{3\text{low}}|^2 - |a_{3\text{high}}|^2 = 0$ , we can reduce this set of four equations for amplitudes to a Hamiltonian set of equations for variables  $w$  and  $\psi$ :

$$\frac{dw}{d\xi} = \frac{\partial H(w, \psi)}{\partial \psi} = -bw^{3/2}(1-w)^{1/2} \sin \psi - 2bw(1-w) \sin 2\psi, \quad (6)$$

$$\frac{d\psi}{d\xi} = -\frac{\partial H(w, \psi)}{\partial w} = -4\omega^2 + \frac{1}{2}b(2w-1)(1+2\cos 2\psi) + \frac{1}{2}bw^{1/2} \left[ \frac{w}{(1-w)^{1/2}} - 3(1-w)^{1/2} \right] \cos \psi,$$

where  $b$  is the total conserved energy;  $w = 2b^{-1}|a_{1\text{low}}|^2$  is the normalised power of the first harmonic;  $\psi = \psi_{3\text{low}} - \psi_{1\text{low}}$  is the effective phase; and

$$H(w, \psi) = 4\omega^2 w + \frac{1}{2}bw(1-w)(1+2\cos 2\psi) + bw^{3/2}(1-w)^{1/2} \cos \psi \quad (7)$$

is the Hamiltonian, which is also conserved in the process of propagation. Recall that such a reduction is possible only in the absence of SRS. Using new variables  $w$  and  $\psi$ , we can define the light field intensity at the point  $\eta = 0$  by the expression  $I(\eta = 0, \xi) = 2b[1 + 2w^{1/2}(1-w)^{1/2} \cos \psi]$ . Equations (6) and (7) provide rather accurate estimates for the compression ratio of the pulse  $Nkcn(\eta, k)$  without direct integration of the Schrödinger equation. In what follows, we define the pulse compression ratio as the ratio of the light field intensity  $I_{\text{opt}}(\eta = 0, \xi = L_{\text{opt}})$  at the point of maximum compression,  $\xi = L_{\text{opt}}$ , to the input intensity  $I_0(\eta = 0, \xi = 0)$ .

Comparing the results obtained in the approximation including a finite number of harmonics with the results of direct numerical integration of the nonlinear Schrödinger equation for the initial conditions  $q_{\text{cn}}(\eta, \xi = 0) = Nkcn(\eta, k)$  in the absence of SRS, we find that these results agree very well within a certain interval of  $k$  values. This interval depends on the wave order  $N$ . Specifically, for  $N = 2$ , the error in determining the compression ratio in the approximation including a finite number of harmonics does not exceed 5% for any  $k \in [0, 0.85]$ . However, the applicability range of this approximation rapidly narrows with increasing  $N$ : for  $N = 4$ , our approximation is applicable within the interval of  $[0, 0.5]$  with the same 5% criterion. Fig. 1a presents the dependence of the pulse compression ratio on the parameter  $k$  calculated by a direct integration of the set (1) in the absence of SRS for several  $N$ . Within the framework of approximation including a finite number of harmonics, the compression ratio is low in the case of a low localisation degree, noticeably increasing with the growth in  $k$  and reaching its maximum value equal to  $\sim 16(N-1)^2/N^2$  for  $k = 1$ .

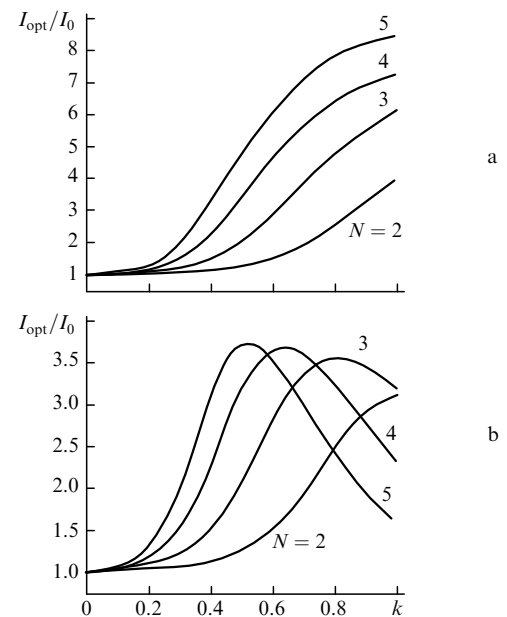


**Figure 1.** Compression ratio  $I_{\text{opt}}/I_0$  for a cn wave as a function of the localisation parameter  $k$  (a) in the absence of SRS and (b) in the presence of SRS for different  $N$ ,  $\mu = 0.001$ ,  $\alpha = 1$ ,  $\delta = 0$ , and  $\sigma = 1.46$ .

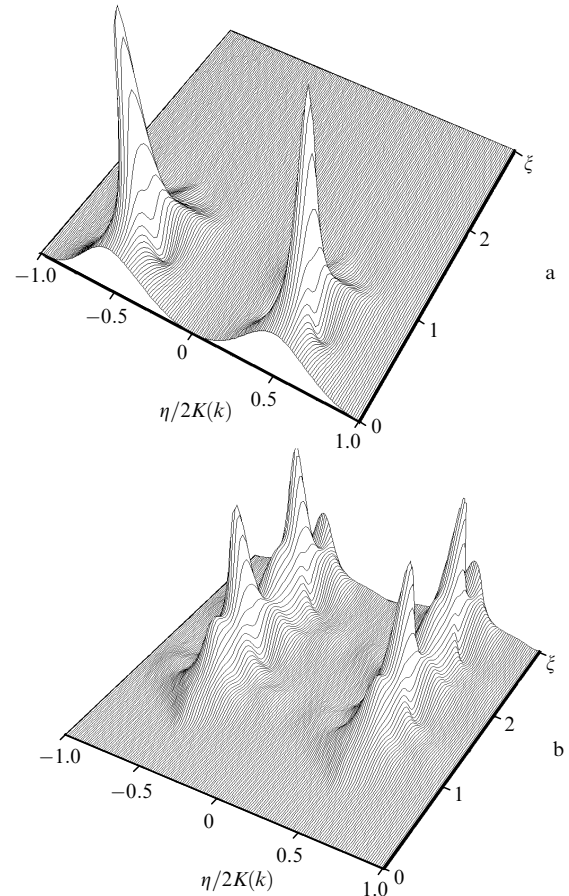
Energy transfer to the signal wave lowers the compression ratio of the pump pulse. The dynamics of wave propagation under these conditions is determined to a considerable extent by the initial amplitude of the signal wave. If this amplitude is sufficiently small, then the pump wave passes through several stages of sequential compression, broadening, splitting into fragments, and recovery of the initial profile before the energy exchange between the waves becomes efficient. We are interested in a situation when the Stokes wave is amplified in an avalanche-like fashion around the point of the first compression of the pump wave. The approximation including a finite number of harmonics is inapplicable in this case, since this approach does not allow self-compression and energy exchange to be included simultaneously. To investigate the influence of SRS on the propagation dynamics of multisoliton cn waves with  $N > 1$ , we performed a direct numerical integration of the set (1).

Fig. 1b displays the compression ratios of the pump pulse as functions of the localisation parameter  $k$  for several values of  $N$  in the regime of group-velocity matching,  $\delta = 0$ . One can see that, while the compression ratio of the pump pulse for  $N = 2$  is virtually the same as in the absence of scattering, high-intensity energy exchange between the waves occurring for  $N = 4$  considerably reduces the compression ratio of the pump pulse. The maximum compression ratio is achieved in the latter case for intermediate values of  $k$  rather than in the limiting case of strong localisation. A typical dynamics of interaction between the signal and pump waves is shown in Fig. 2 for  $N = 3$  and  $k = 0.8$ . Energy exchange between these waves results in the formation of an approximately three-soliton signal wave. The compression ratio of the signal pulse, defined as the ratio of the intensity of the signal wave at the point of maximum compression to the input intensity of the pump wave, is always somewhat lower than the compression ratio of the pump pulse in the absence of SRS (Fig. 1a).

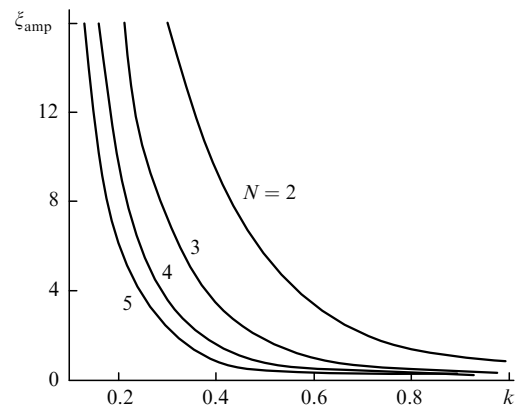
The dynamics of wave interaction in the limiting case of strong spatial localisation is also of considerable interest. If energy exchange between the waves is especially efficient at the distance  $\xi \approx 3\pi/16$ , when the pump pulse is split into two fragments and the sweeping rate of the frequency  $\partial\omega_s/\partial\eta$  has its maximum value, then two diverging pulses are produced at the Stokes frequency. If energy exchange occurs at the distance  $\xi \approx \pi/4$ , when the pump pulse still consists of two fragments and the frequency sweeping rate reaches its minimum, then a bound state of solitons is produced instead of a pair of diverging pulses.

Fig. 3 displays the distance  $\xi_{\text{amp}}$  corresponding to 50% energy conversion from a cn pump wave into the signal wave as a function of the localisation parameter  $k$  for several values of  $N$ . One can see that the distance  $\xi_{\text{amp}}$  infinitely increases for  $k \rightarrow 0$  due to the fact that the intensity of the pump wave and, consequently, the intensity of energy exchange are proportional to  $k^2$ . One can also easily notice that a growth in  $N$  leads to a substantial increase in the intensity of energy exchange. Note also that, even for  $N = 5$ , the distance  $\xi_{\text{amp}}$  becomes virtually independent of  $k$  for  $k > 0.6$ . In addition, in the limiting case of strong spatial localisation,  $\xi_{\text{amp}}$  only slightly depends on  $N$  for  $N \geq 5$ .

Group-velocity mismatch plays an important role in the generation of a Stokes signal. As shown in [9], the efficiency of energy exchange between the pulses in the limiting case of strong spatial localisation considerably lowers with the increase in the group-velocity mismatch [the growth in the



**Figure 2.** Dynamics of (a) cn pump wave and (b) signal wave for  $N = 3$ ,  $k = 0.8$ ,  $\mu = 0.001$ ,  $\alpha = 1$ ,  $\delta = 0$ , and  $\sigma = 1.46$ .



**Figure 3.** Dependence of the distance  $\xi_{\text{amp}}$  on the localisation parameter  $k$  in the case of an SRS of a cn wave for different  $N$ ,  $\mu = 0.001$ ,  $\alpha = 1$ ,  $\delta = 0$ , and  $\sigma = 1.46$ .

parameter  $\delta$  in Eqn (1)]. This is due to the fact that the pulse being amplified (lagging behind the pump pulse in the regime of anomalous dispersion) leaves the area of efficient amplification, where the intensity of the pump pulse has its maximum value. A radically different situation is observed in the case of an SRS of a *periodic* cnoidal wave. Due to its periodicity, the signal wave ‘drifting’ with respect to the pump wave may meet the conditions of optimal amplifications for certain values of  $\delta$  and the period. This may be manifested, in particular, in a nonmonotonic dependence of

the distance  $\xi_{\text{amp}}$  on the group-delay parameter  $\delta$  (Fig. 4a). For sufficiently large  $\delta$ , the distance  $\xi_{\text{amp}}$  becomes independent of  $\delta$ . Another important effect related to the influence of the group-velocity mismatch on SRS dynamics is the appearance of a permanent component in the spectrum of the Stokes wave, indicating the possibility of generating waves of the dn type.

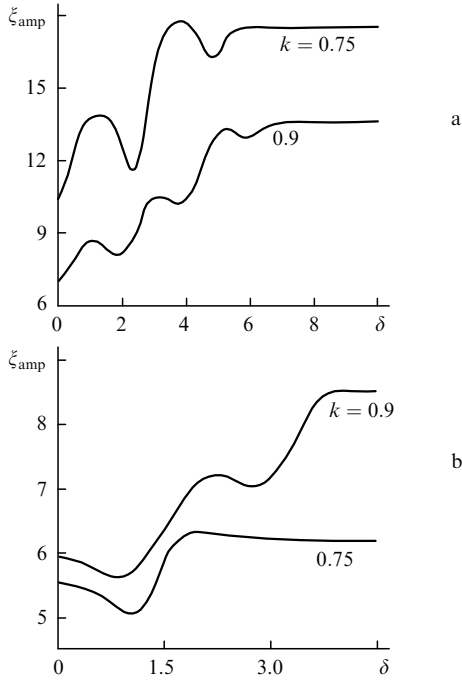


**Figure 4.** Dependence of the distance  $\xi_{\text{amp}}$  on the group-delay parameter  $\delta$  for (a) a cn and (b) dn wave with  $\mu = 0.001$ ,  $\alpha = 1$ ,  $\sigma = 1.46$ , and  $N = 3$ .

#### 4. Self-compression and SRS of a dn wave

The dynamics of SRS of a dn wave is much more complicated than the dynamics of SRS of a cn wave because of the presence of a permanent component in the spectrum of a dn wave, which is seen from the Fourier spectrum of a dn wave:

$$N\text{dn}(\eta, k) = \frac{N\pi}{2K(k)} + \frac{2N\pi}{K(k)} \sum_{m=1}^{\infty} g^m (1 + g^{2m})^{-1} \cos \frac{\pi m}{K(k)} \eta. \quad (8)$$

In the limiting case of low localisation, a dn wave can be considered as a plane wave with a superimposed small harmonic perturbation. Analysis of the self-compression of a dn-wave pulse in the absence of SRS in the approximation including a finite number of harmonics by using the Hamiltonian formalism gives the most reliable results for  $N = 2$ , since only harmonics with  $m = 1$  [with frequencies  $2\omega_1 = \pm \pi K^{-1}(k)$ ] in the expansion (8) fall within the frequency band of modulation instability of the zeroth harmonic (the plane wave) and determine the nonlinear dynamics of the system. The wave field in this case is written as

$$q(\eta, \xi) = a_{\text{low}}(\xi) \exp(-i2\omega_1\eta) + a_0(\xi) + a_{\text{high}}(\xi) \exp(i2\omega_1\eta). \quad (9)$$

The wave described by Eqn (9) contains more than 95 % of energy of the corresponding dn wave for  $k = 0 - 0.95$ .

Substituting Eqn (9) into the nonlinear Schrödinger equation and equating the terms with equal frequencies, we arrive at a set of three coupled equations for harmonic amplitudes. Using the law of conservation of energy,  $|a_{\text{low}}|^2 + |a_0|^2 + |a_{\text{high}}|^2 = b = \text{const}$ , and the difference of absolute values of harmonic amplitudes squared,  $|a_{\text{low}}|^2 - |a_{\text{high}}|^2 = 0$ , we can reduce this set of equations to a set of Hamiltonian equations for variables  $w$  and  $\psi$ :

$$\frac{dw}{d\xi} = \frac{\partial H(w, \psi)}{\partial \psi} = -2bw(1-w) \sin \psi, \quad (10)$$

$$\frac{d\psi}{d\xi} = -\frac{\partial H(w, \psi)}{\partial w} = -4\omega_1^2 + b(3w-1) + 2b(2w-1) \cos \psi,$$

where  $b$  is the total conserved energy;  $w = b^{-1}|a_0|^2$  is the normalised power of the zeroth harmonic;  $\psi = \psi_{\text{low}} + \psi_{\text{high}} - 2\psi_0$  is the effective phase. The Hamiltonian of the set (10) is written as

$$H(w, \psi) = 4\omega_1^2 w + bw(1-1.5w) + 2bw(1-w) \cos \psi. \quad (11)$$

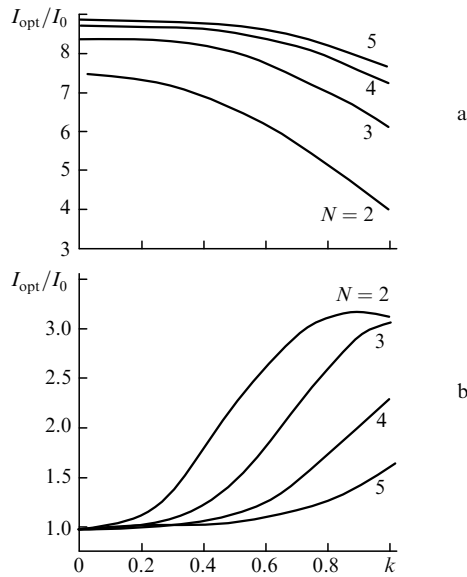
Using new variables, we can represent the light field intensity at the point  $\eta = 0$  as  $I(\eta = 0, \xi) = b(2-w) + 2^{3/2}bw^{1/2}(1-w)^{1/2} \cos \psi$ .

Comparing the results obtained in the approximation including a finite number of harmonics with the results of direct numerical integration of the nonlinear Schrödinger equation for the initial conditions  $q_{\text{dn}}(\eta, \xi) = 2\text{dn}(\eta, k)$  in the absence of SRS, we find that the approximation including a finite number of harmonics provides a sufficiently high accuracy in predicting the point of maximum compression (with an error not exceeding 5%). However, this approximation is much less accurate in predicting the compression ratio (the error may be  $\sim 30\%$  in this case).

Fig. 5 presents the compression ratio of a dn wave as a function of the localisation parameter  $k$  calculated by a direct integration of the set (1) in the absence of SRS for several values of  $N$ . Note that the compression ratio of the dn wave in the absence of scattering reaches its maximum for  $k \rightarrow 0$ . The amplitudes of the first and higher order harmonics are small in this case, which slows down the build-up of modulation instability, resulting in self-compression. Therefore, we have  $L_{\text{opt}} \rightarrow \infty$  for  $k \rightarrow 0$ . The range of  $k$  values where the compression ratio remains virtually constant broadens with the increase in the wave order  $N$ .

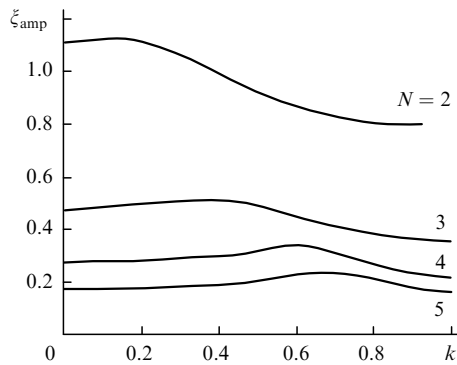
The inclusion of SRS radically changes the scenario of self-compression of the pump pulse. Fig. 5b displays the compression ratio of the pump pulse as a function of the localisation parameter  $k$  for several values of  $N$ . Since the amplitudes of the first and higher order harmonics are small for  $k \rightarrow 0$  (i.e., the modulation instability is suppressed), while the amplitude of the zeroth harmonic is large (resulting in an efficient energy exchange with the signal wave already at the initial stage of propagation), considerable compression ratios cannot be achieved in the limiting case of weak localisation because of fast pump depletion. In contrast to Fig. 5a, the compression ratio increases in this regime with the growth in  $k$  and lowers with the increase in the wave order  $N$ .

Fig. 6 displays the distance  $\xi_{\text{amp}}$  corresponding to 50 % energy conversion from a dn pump wave into the signal wave as a function of the localisation parameter  $k$  for



**Figure 5.** Compression ratio  $I_{\text{opt}}/I_0$  for a dn wave as a function of the localisation parameter  $k$  (a) in the absence of SRS and (b) in the presence of SRS for different  $N$ ,  $\mu = 0.001$ ,  $\alpha = 1$ ,  $\delta = 0$ , and  $\sigma = 1.46$ .

several values of  $N$ . As can be seen from this figure, the distance  $\xi_{\text{amp}}$  for a dn wave, in contrast to the case of a cn wave, only slightly changes with the growth in the localisation parameter  $k$  and rapidly decreases with the growth in  $N$ . Numerical integration shows that, even for  $N \sim 8$ , the distance  $\xi_{\text{amp}}$  becomes virtually independent of  $k$  for  $k < 0.9$ .



**Figure 6.** Dependence of the distance  $\xi_{\text{amp}}$  on the localisation parameter  $k$  in the case of an SRS of a dn wave for different  $N$ ,  $\mu = 0.001$ ,  $\alpha = 1$ ,  $\delta = 0$ , and  $\sigma = 1.46$ .

Specific features of the formation of the signal wave in SRS of a dn wave are associated with the fact that an efficient energy exchange occurring at the initial stage of propagation within the areas of the maximum intensity of the pump wave leads to the formation of narrow peaks in the signal wave. At subsequent stages, however, the energy exchange between the signal and pump waves within the areas of minimum pump intensity (where the pump intensity is, nevertheless, nonzero due to the permanent component of the pump wave) gives rise to a complicated additional structure of the field between the narrow peaks of the signal wave. Subsequently, the dynamics of the signal wave becomes even more complicated due to the competition of dispersion effects and self-focusing.

In addition, while the scattering of a fundamental dn wave with  $N = 1$  gives rise to a zeroth harmonic in the spectrum of the signal wave, no zeroth harmonic is observed in the spectrum of the signal wave in the case of scattering of waves with  $N > 1$ . Note also that the maximum compression ratio of signal and pump pulses in the above-considered case is always lower than the compression ratio of a dn-wave pulse in the absence of SRS. Similar to the case of a cn wave, the inclusion of group-velocity mismatch results in a non-monotonic dependence of the distance  $\xi_{\text{amp}}$  on the group-delay parameter (Fig. 4b) and leads to the appearance of a zeroth harmonic in the spectrum of the signal wave.

## 5. Conclusions

Thus, SRS of multisoliton cnoidal pump waves results in the formation of high-intensity cnoidal waves at the Stokes frequency. These signal cnoidal waves consist of a sequence of narrow peaks without broad pedestals. The compression ratio of a cn-wave pulse in the absence of SRS monotonically increases with the increasing localisation parameter  $k$ . The maximum compression ratio of a dn wave in the absence of SRS is achieved for  $k \rightarrow 0$ . As  $k$  increases, the compression ratio of a dn-wave pulse monotonically lowers. Stimulated Raman scattering also decreases the compression ratio of the pump pulse. The maximum compression ratios of both cn and dn waves in this case are achieved for intermediate values of the localisation parameter  $k$ . Group-velocity mismatch results in a nonmonotonic dependence of the distance of Stokes-wave excitation on the group-delay parameter and the localisation parameter of the wave-field energy, giving rise to the appearance of a zeroth harmonic in the spectrum of the signal wave.

## References

1. Vysloukh V A, Petnikova V M, Shuvalov V V *Kvantovaya Elektron.* **25** 1062 (1998) [*Quantum Electron.* **28** 1034 (1998)]
2. Vysloukh V V, Petnikova V M, Rudenko K V, Shuvalov V V *Kvantovaya Elektron.* **28** 55 (1999) [*Quantum Electron.* **29** 613 (1999)]
3. Petnikova V, Shuvalov V, Vysloukh V *Phys. Rev. E* **60** 1 (1999)
4. Aleshkevich V, Vysloukh V, Kartashov Y. *Opt. Commun.* **173** 277 (2000)
5. Ankiewicz A, Krolikowski W, Akhmediev N *Phys. Rev. E* **59** 6079 (1999)
6. Mollenauer L, Stolen R, Gordon J, Tomlinson W *Phys. Rev. Lett.* **45** 1095 (1980)
7. Mollenauer L, Stolen R, Gordon J, Tomlinson W *Opt. Lett.* **8** 289 (1983)
8. Gordon J *Opt. Lett.* **8** 596 (1983)
9. Vysloukh V A, Serkin V N *Pis'ma Zh. Eksp. Teor. Fiz.* **38** 170 (1983) [*JETP Lett.* **38** 170 (1983)]
10. Vysloukh V A, Serkin V N *Izv. Akad. Nauk SSSR Ser. Fiz.* **48** 1777 (1984)
11. Smith R *Appl. Opt.* **11** 2489 (1972)